DOI 10.1007/s10946-024-10203-8
Journal of Russian Laser Research, Volume 45, Number 2, March, 2024

HANDLING DISTURBANCE IN OPTICAL BEAM ALIGNMENT USING THE MPC APPROACH

Ammar Ramdani,[1*] Mohamed Traïche,[1] and Said Grouni[2]

[1] *Center for Development of Advanced Technologies (CDAT)*
OP17, City 20 August 1956, Baba Hassen 16303, Algiers, Algeria

[2] *Industrial Maintenance Department, University of Tamanghasset*
Tamanrasset 11000, Algeria

*Corresponding author e-mail: aramdani@cdta.dz

Abstract

Optical systems, such as a mobile LiDAR system, encounter mechanical disturbances associated with the condition of the road, resulting in significant misalignments in the optical paths within the system. To address this issue, considerable time is dedicated to the realignment process to restart the system. A suggested approach to overcome this challenge involves the implementation of automatic realignment through the control of the motion of the steering mirrors using an advanced control technique known as Model Predictive Control (MPC). This technique, which is relatively new in the field of optics, is widely utilized in the industry due to its capability to manage and resolve a broad range of problems that are inherent to industrial systems, particularly, those that are subject to constraints or undergo disturbances during operation. In this study, we utilize MPC on the optical chain, specifically the LiDAR component, to regulate the beam and promptly rectify any flexure that occurs during both constant and variable trajectories, as well as in the presence of disturbances. A comparative analysis is conducted with the PID controller to evaluate the performance of the advanced technique proposed.

Keywords: optical beam alignment, dynamic matrix control, Skogestad internal model control, noise, disturbance.

1. Introduction

Model Predictive Control (MPC) is an advanced control strategy [1], its field of application extends to all industrial areas [2], even in clinical and biomedical fields; it is considered as one of the most important controlling strategies [3]. The MPC-MISO model for the depth of simultaneous co-administration of the hypnotic and analgesic drugs and their effect on the Bispectral Index Scale (BIS) was analyzed to provide the optimum dosage for the desired BIS level, taking into account constraints [4]. Under the event-based adaptive horizon, the MPC was proposed to study the trajectory tracking of marine surface vessels [5], to follow the reference attitude trajectories of an aerospace vehicle subject to constraints and uncertainties [6], for the optimum charging of a Li-ion battery [1], and to study the effect of prediction and control the horizon parameters [7]. The effectiveness of the Model Predictive Control (MPC) closed-loop identification without excitation was demonstrated to improve the control performance [8]. The closed-loop dynamics of linear systems under approximate MPC, using a finite number of Alternating Direction Method of Multiplier (ADMM) iterations per time step, was studied to investigate the performance of the MPC and offer practical guidance for its implementation in real-world applications [9]. A Dynamic

Manuscript submitted by the authors in English on December 11, 2023.

Real-Time Optimization formulation with closed-loop prediction was proposed to coordinate distributed model predictive controllers (MPCs) aiming to improve performance in both target tracking and economic optimization [10]. A novel MPC algorithm that eliminated the need for terminal constraints and costs was presented, resulting in a reduced prediction horizon, while maintaining stability and robustness properties [11].

An Improved Model Predictive Direct Torque Control (IMPDTC) algorithm considered multi-step delay compensation to address the issues of torque and stator flux pulsation in squirrel cage induction motors. It aimed to minimize the deviation between the optimum voltage vector and the reference values of stator flux linkage and torque, while also studying a measure to solve the delay problem in digital control systems [12]. This IMPDTC method was proposed for a variable speed converter, selecting the optimum switching state of the converter to minimize the error between predicted and computed values of torque, flux, and reactive power components, using PSO optimization to optimize the weighting factors for the control method [13]. An indirect MPC approach was proposed for a modular multilevel converter connected to a high-voltage direct current bus line, to transfer active power bi-directionally to the grid and compensate reactive power [14]. An energy collaborative optimization management approach for an energy storage system (ESS) of a Virtual Power Plant (VPP), using model predictive control (MPC), was studied. It utilized a long–short-term memory (LSTM) neural network to obtain one-hour-ahead forecasting information for the load, wind generation, and photovoltaic generation to minimize the economic cost of the VPP [15].

The Dynamic Matrix Control (DMC) was employed to study thermal conditions in the infant incubator for premature babies [3]. It was used with an improved sliding mode for controlling the loading and measuring system of a spindle [16], for a networked system that addresses the challenges of time delay, packet loss, and disturbed sequence [17], with delays and large inertia demonstrated [18]. It was proposed to control objects with integrals and delay links addressing the deficiencies of traditional control methods and improving control quality [19].

An automatic alignment technique was developed, employing Global Positioning System (GPS), to make use of the signal power returned to perform the fine alignment [20]. The technique, based on photodiodes and the use of differential phase modulation, allowed the detection of the phase difference between two Gaussian beams of an interferometer [21]. It is appropriate to analyze the effects of optical cavity misalignment [22] and to realize its optimum performance [23]. The influence of alignment error on the coupling efficiency, beam quality, and beam power distribution of a Gaussian beam for multimode fiber was studied in [24]. The research conducted in this study concentrated on the alignment of the optical chain, a crucial step in the LiDAR system. This system, which was housed in a moving van, was subjected to vibrations resulting from mechanical strains associated with the condition of the road (such as speed bumps and potholes) and rugged terrains, which, in turn, disrupted the optical alignments of the system. Recognizing that the realignment process takes a considerable amount of time, measured in hours, the proposed solution entailed the dynamic management of these alignments to compensate for them in realtime. This was achieved through the electronic control of stepper motors, which secured the supports of the optical components. The stepper motors rotate the laser beam at an angle of approximately 0.01 mrad. Their electronic control was executed in a closed loop, using light sensors positioned laterally to the propagation axis, which received a portion of the light emitted by the laser beam. The automatic alignment of the optical chain represents a significant advantage of our system compared to other studies that still rely on manual alignment, such as the mobile LiDAR systems developed in South Africa, focusing on the atmosphere [25], or those employing optical scanners to investigate aerosols [26] and clouds [27]. A

similar case could be observed in a mobile LiDAR system autonomously controlled under the LabVIEW platform developed by Swedish researchers [28]. Hence, the automatic alignment enables us to save time in preparing the system for operation after each trip, given that we are dealing with a mobile system that needs to quickly adapt to various road conditions. The entire system was utilized for the detection of forest fires and the analysis of the atmosphere [29].

The research presented in this study aims to contribute to the field by introducing an innovative approach to controlling the optical chain in the LiDAR system. The primary objective is to ensure the optimum movement of the optical supports, which are responsible for rotating the optical beam and scanning a specific area. This task becomes particularly challenging, when considering the presence of external disturbances and the need to maintain the desired set point or reference value. To address this problem, we employ an advanced Predictive Control technique, which not only helps in solving the disturbance issue but also saves time through quick automatic alignment. The optical chain comprises the mirror support and two stepper motors, which enable the movement of the laser beam. This beam is generated by a laser source and is used for various purposes, such as fire detection or analyzing the atmosphere in polluted environments near industrial sources. In this study, we thoroughly discuss the LiDAR application's synoptic scheme. The research primarily focuses on controlling the optic chain system, using advanced Model Predictive Control (MPC) and Proportional Integral Derivative (PID) techniques. Specifically, the rotation of the optical chain in the LiDAR system is controlled, using a novel technique developed from a prediction model that utilizes the step response to obtain an optimum solution by minimizing a quadratic criterion. The simulation results compare the performance of the MPC technique with the SIMC-PID controller proposed by Skogestad [30] in terms of tracking accuracy and disturbance rejection. The ultimate goal of the control system is to maintain the desired behavior and achieve the desired set point or reference value, even in the presence of external influences.

This paper is organized as follows.

Section 2 entails the creation of the optical chain model, a component of the LiDAR application. In Sec. 3, we develop the Dynamic Matrix Control (DMC) technique, which encompasses the prediction model, prediction horizon, control horizon, receding horizon control, and synthesis of the DMC technique. In Sec. 4, we present the findings and a discussion of the proposed technique, along with practical outcomes. Finally, we conclude the paper in Sec. 5.

2. Design of the Optical Chain Model

2.1. Optical Chain of the LiDAR Application

The alignment optics employed in our investigation comprises multiple deflection mirrors, each of which is produced by applying a layer of gold onto a metal disk with a diameter of 30 mm. The angular rotation, denoted as θ, of each mirror results in a corresponding rotation of the beam by an angle of $2\,\theta$. In Fig. 1, we depict a beam expander (alternatively referred to as a collimator) as an integral component of the transmission optics. This particular element serves the purpose of diminishing the divergence of the laser beam to a magnitude of a few tenths of a milliradian, thus enabling enhanced precision in directing the beam over significant distances.

The laser beam, being discharged, is aimed toward a designated target (smoke) and is then redirected back from this target through backscattering. The arrangement of the telescope; see Fig. 1, is referred to as Newtonian. It is of particular interest in cases involving stationary systems. The returning signal within

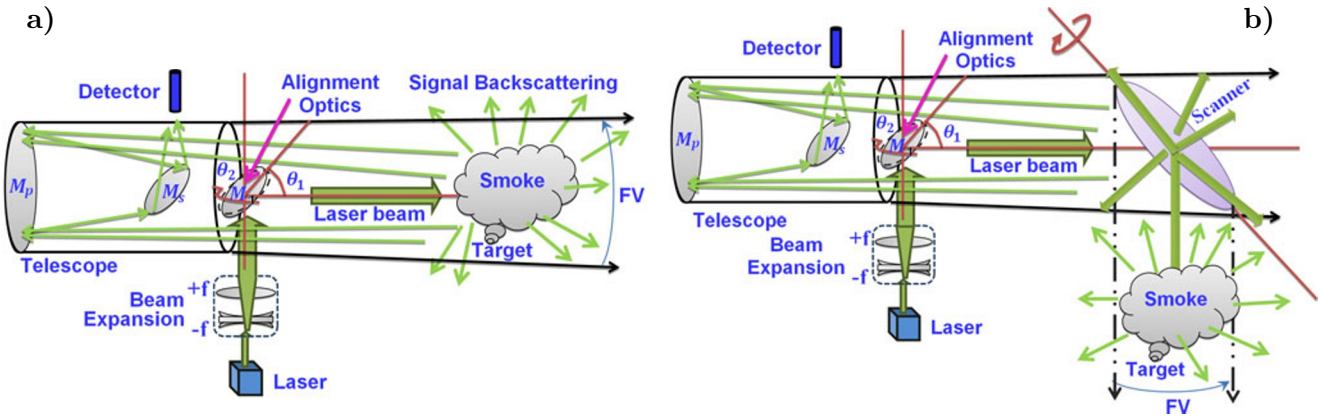

Fig. 1. Synoptic scheme of the LiDAR application with the elements: the laser, optical chain, telescope with a detector, and target (a); the same elements with a scanner (b). Here, FV is the field of view of the telescope, M_p is a primary mirror, and M_s is a secondary mirror.

the telescope's field of view (measured in solid angle) is collected and intensified by its primary mirror, and subsequently directed towards the secondary mirror, which then reflects it towards the detector. In Fig. 1 a, the diagram indicates that the telescope's field of view, along with the laser beam, possesses a fixed orientation. However, in actual practice, we employ the diagram shown in Fig. 1 b, wherein a sizable scanner mirror is incorporated to facilitate the rotation of the laser beam and the telescope's field of view, ensuring that they remain in alignment throughout the rotation. This enables the search for targets, whose positioning is initially unknown. This investigation aims to achieve the alignment of the emitted laser beam in such a manner, that it consistently remains coaxial with the telescope's segment 3; see Fig. 1 b. To accomplish this, we manipulate the mirrors M_1 and M_2 at extremely minute angles. The execution of this operation must be automated.

2.2. Parameters of the Optical Chain Model

On each segment of the laser beam alignment, it is necessary to position the beam splitter BS, which reflects a fraction of the beam towards a network of luminescence sensors Sij, arranged in a 3×3 matrix; see Fig. 2. This arrangement enables the prompt identification and adjustment of misaligned components within the system.

The model system comprises a mirror that is adjusted through rotation in both right and left directions, as well as up and down directions, and reciprocally through handles; see Fig. 3 a. This adjustment is carried out by controlling its support, which includes micrometric

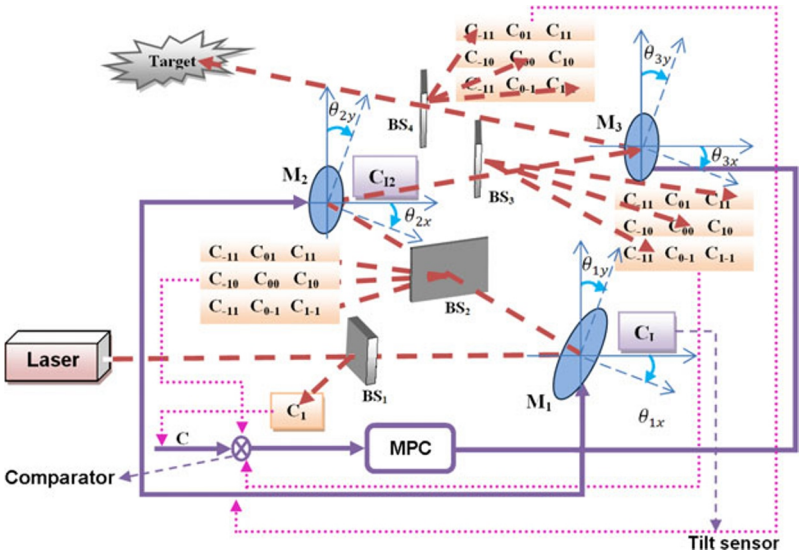

Fig. 2. Diagram of mirror's control.

a) 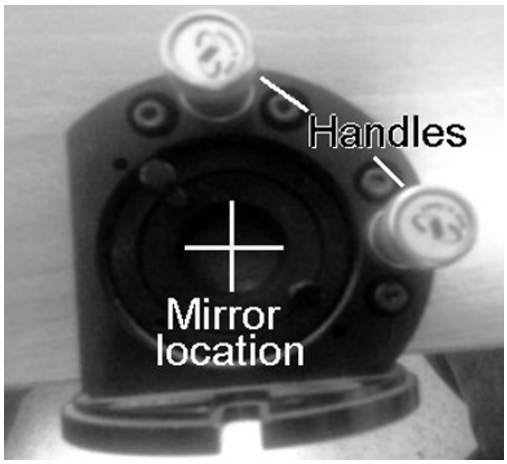

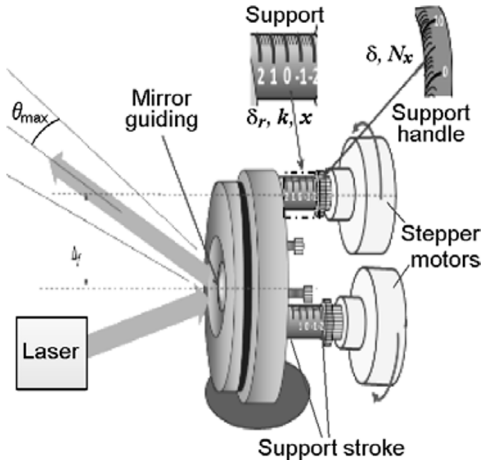

b)

Fig. 3. The mirror support to be controlled (a) and graduated scales quantifying the rotation of the mirror (b).

translators that convert linear motion into rotation; see Fig. 3 b. The equations of the model can be found in Sec. 4.

3. Dynamic Matrix Control (DMC) Technique Characteristics

Dynamic Matrix Control (DMC) possesses certain distinctive features that set it apart from other control strategies. These characteristics of DMC contribute to its effectiveness and make it a popular choice in various industrial applications. DMC is known for its ability to handle systems with multiple inputs and outputs, allowing for the control of complex processes. Additionally, DMC is highly adaptable and can be easily customized to suit specific system requirements. This versatility enables DMC to effectively control a wide range of processes, from simple to highly complex ones. The dynamic nature of DMC allows it to continuously update its control actions based on realtime data, ensuring optimum performance and stability. Furthermore, DMC employs a predictive control approach, which means that it takes into account future system behavior and makes control decisions accordingly. This proactive approach enhances the ability of DMC to respond quickly and accurately to system disturbances and changes. The mathematical model used in DMC is based on a dynamic matrix, which represents the relationship between inputs, outputs, and process dynamics. By utilizing this matrix, DMC can calculate the optimum control actions that will minimize process deviations and achieve the desired set point. Overall, the characteristics of DMC make it a powerful and flexible control strategy that can effectively handle a wide range of industrial processes.

3.1. Prediction Model

Dynamic Matrix Control (DMC) utilizes the representation of the step response to forecast, both the input and output. Its industrial accomplishments are attributed to its proficiency in managing constraints and disturbances for large-scale multivariate systems [31,32]. The system's step response can be described as follows:

$$y(t) = \sum_{i=1}^{+\infty} g_i \Delta u(t-i). \tag{1}$$

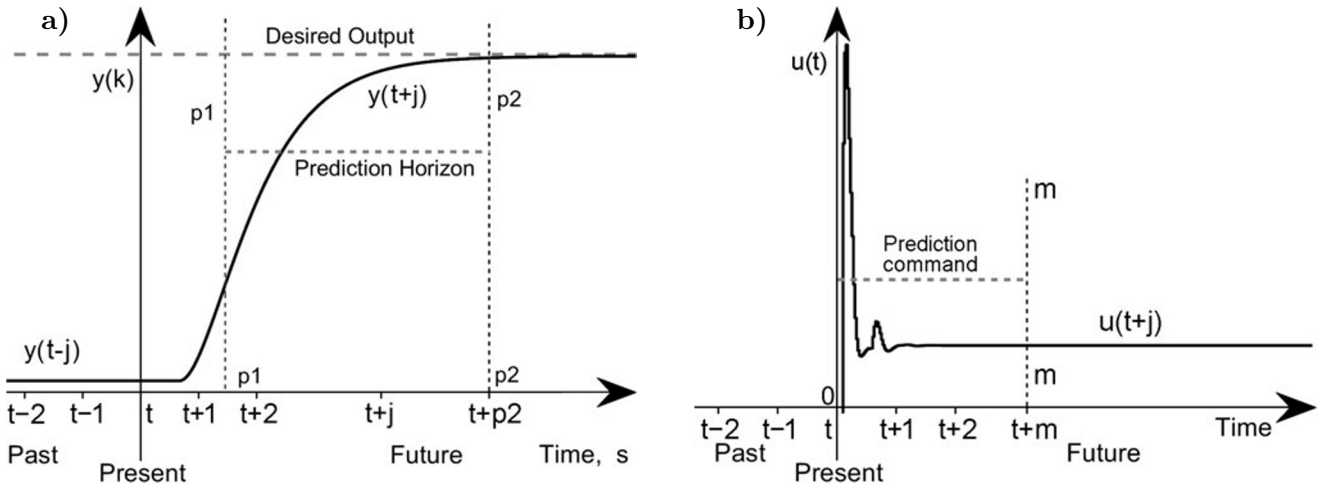

Fig. 4. Principle of the prediction horizon (a) and the control horizon (b).

The system's step response is produced by the application of a unit step; see Fig. 4. The variable $u(t)$ denotes the control input at time t and serves to portray the system's reaction to a step input. The command increment $\Delta u(t)$ symbolizes the alteration in the control input from its preceding value to its present value at time t, with

$$u(t) = \begin{cases} 0 \ \forall \ t < 0, \\ 1 \ \forall \ t \geq 0. \end{cases} \tag{2}$$

The model output, denoted as $y(t)$, is influenced by the coefficient of the step response g_i. Additionally, the increment control Δu plays a role in the prediction of the output system at the instant $(t + k)$,

$$\hat{y}(t+k) = \sum_{i=1}^{k} g_i \Delta u(t+k-i) + \sum_{i=k+1}^{+\infty} g_i \Delta u(t+k-i) + \hat{\eta}(t+k). \tag{3}$$

Since $\hat{\eta}(t+k)$ is the predicted disturbance at $(t+k)$, it reads

$$\hat{\eta}(t+k) = \hat{\eta}(t) = y_m(t) - y(t). \tag{4}$$

The predicted output can be expressed as

$$\hat{y}(t+k) = \sum_{i=1}^{k} \Delta g_i \Delta u(t+k-i) + \sum_{i=k+1}^{+\infty} g_i \Delta u(t+k-i) + y_m(t) - \Delta_{i=1}^{k} g_i \Delta u(t-i), \tag{5}$$

or

$$\hat{y}(t+k) = \sum_{i=1}^{k} g_i \Delta u(t+k-i) + f_u(t+k). \tag{6}$$

3.2. Prediction Horizon [p1 and p2]

MPC operates by predicting the system's future behavior over a defined prediction horizon. The prediction horizon represents a time span into the future, and the system's response is estimated for that duration. The finite time interval, from which the output is expected, is referred to as the output prediction horizon. The evolution of this interval begins at the lower prediction component p1, and

progresses towards the upper prediction part p2 of the output. Thus, the length of this interval is influenced by factors, such as the speed or slowness of the gadget and whether it is delayed or not, among others.

If the time delay d is exactly known, there is no need to put in p1 unless d, because it would then be useless calculations in the corresponding output, which cannot be affected by the first action $u(t)$. If d is not known or is variable, then p1 can be set to 1. The final (maximum) prediction horizon p2 depends on both the open loop response time and the sampling time T_s. Specifically, p2 is determined to be equal to the Closed Loop Response Time (CLRT) divided by the sampling time p2$\leq$CLRT/$\mathrm{T_S}$. It should be noted that the larger p2, the longer the computing time; see Fig. 4 a.

3.3. Control Horizon [m]

The control horizon, denoted as m, is a subset of the prediction horizon and represents the time span, for which control actions are explicitly determined. Typically, only the first control action is implemented, and the optimization problem is repeatedly solved at each control step. For simple processes, the control horizon m is taken to be equal to one; on the other hand, for complex processes, m must be at least equal to the number of unstable or poorly damped poles. Under no circumstances, should the control horizon be larger than the maximum forecast horizon; in other words, m should be either smaller or equal to p2 ($m \leq$ p2); see Fig. 4 b. A value of m equal to one is commonly used for achieving generally applicable control. By applying these two rules to specific systems, accurate results can be obtained. Furthermore, alternative approaches can also be employed. The aforementioned guidelines are commonly used in the calculation of process control and output [33–35],

$$5 \leq m \leq 20, \tag{7}$$

$$\mathrm{p} = N + m. \tag{8}$$

The coefficients of the step response of the process model denoted as N are typically selected as follows:

$$30 \leq N \leq 120. \tag{9}$$

3.4. Receding Horizon Control

MPC employs a receding horizon control strategy, also known as a moving horizon control. At each control step, the optimization problem is solved over the prediction horizon, but only the first control action is applied. The optimization problem is then solved again at the next control step, considering updated measurements and states.

3.5. Synthesis of the DMC Algorithm

The primary aim of a DMC controller is to steer the output toward the desired set point, with utmost precision by employing a least-squares approach. It is also possible to integrate a penalty term on the input moves, thereby enhancing the controller's overall performance. Accordingly, the manipulated variables are carefully chosen to minimize a quadratic objective function, that takes into account the reduction of future errors and incorporates the control effort. This results in the controller adopting a generic form [36],

$$J(p_1, p_2, m) = \sum_{j=p_1}^{p_2} \left[\hat{y}(t+j) - w(t+j)\right]^2 + \lambda \sum_{j=1}^{m} \left[\Delta u(t+j-1)\right]^2, \tag{10}$$

where $\hat{y}(t+j/t)$ is the predicted output, with (p1, p2) being the minimum and maximum values of the prediction horizon, m is the value of the control horizon (more details are given above), and $w(t+j)$ is a set point or reference path at a time $(t+j)$; by assumption, it reads

$$w(t+k) = \alpha w(t+k-1) + (1-\alpha)C(t+k). \tag{11}$$

Here, $C(t+k)$ is the set point, which is constant with a value of $\alpha = 0$ (α can vary from 0 to 1), and a small value of α provides a quick reference to its set point C. The coefficient λ, being the weighting coefficient of the control signal, is an important parameter that allows to give more or less weight to the control and the output, to ensure convergence, when the starting system presents a risk of instability. Also, $\Delta u(t+j-1)$ is the command increment at the instant $(t+j-1)$.

The optimum solution is obtained by derivation of the matrix form concerning control vector increments, it reads

$$\Delta u_{\text{opt}} = (G^T G + \lambda I)^{-1} G^T (w - f), \tag{12}$$

where Δu is a column vector, G is a matrix, f and w are vectors, λ is a scalar, I is the identity matrix, and Δu_{opt} are the values that minimize J. The derivative is taken with respect to the vector Δu, and the result is a vector equation, where J is minimized.

So, the values of Δu_{opt} that minimize J are given by the following expression:

$$\Delta u_{\text{opt}}(t) = K_1(w - f), \tag{13}$$

with K_1 representing the first row of the matrix K,

$$K = (G^T G + \lambda I)^{-1} G^T. \tag{14}$$

Therefore, the values of Δu_{opt} that minimize J are given by the above expression. The predicted future control sequence is

$$u(t) = u(t-1) + K_1(f - w). \tag{15}$$

Through utility of the precept of the moving horizon, as in other predictive control strategies, only the first sequence of the control, which makes use of the primary line of the matrix $(G^T G + \lambda I)^{-1} G^T$, is implemented and sent to the process. The calculation is repeated at the subsequent time to have the brand new command u at time $t+1$.

4. Results and Discussion

To demonstrate its efficacy, the Model Predictive Control (MPC) technique is employed on a system comprised of a support and a mirror for regulating its rotation. This particular system, which serves as one of the constituents in the optical chain of Light Detection and Ranging (LiDAR), can be represented by Eq. (16) given below. Within this simulation, we examine various scenarios including a constant trajectory (as shown in Fig. 1), a variable trajectory (as illustrated in Fig. 2), and the presence of disturbances (as shown in Figs. 8 and 5) to assess the capability of the proposed controllers to maintain the desired output and achieve satisfactory performance. The external disturbance signals manifest themselves at sample 700 and persist for a duration of 100 samples; see Fig. 8, thereby influencing the behavior of the system and causing oscillations in the response that reach a magnitude of 16 before being attenuated and eventually eliminated by the proposed controllers. This system possesses the ability to effectively manipulate the orientation of the laser within a solid angle that encompasses a square section, spanning from -112 to $+112$ mrad.

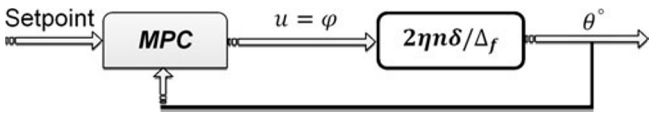

Fig. 5. Synoptic scheme of the closed-loop mirror control for a single variable, with the MPC.

The mirror transfer function [37], as shown in Fig. 3 b, is defined as follows:

$$H(t) = \frac{2n\delta}{\Delta_f} n(t), \tag{16}$$

$$K_p^{'} = \frac{2\eta\delta}{\Delta_f}\,. \tag{17}$$

In Fig. 5, we illustrate the closed-loop mirror control, utilizing the MPC controller. The η relationship between the motor's rotation division and the support division of the micrometric table reads

$$\eta = N_s/N_m = 0.25, \tag{18}$$

with $N_m = 200$ steps and $N_s = 50$ steps, where N_m is the number of steps per motor revolution, and N_s is the number of steps/revolution of the support handle, θ is a mirror alignment position (angle of the beam rotation), φ is the angle of rotation motor (input), δ is the support translation subdivision $\delta = 0.01$ mm, Δ_f is the distance between the mirror's axis of rotation and the axis of attachment of the handle measured in millimeters; $\Delta_f = 35$ mm, and n is an integer that defines the number of motor rotation steps. Thus,

$$H(s) = n \cdot 0.005/s \qquad \text{and} \qquad H(z) = n \cdot 0.0005/(z-1). \tag{19}$$

The discrete transfer function $H(z)$ possesses a sampling time T_s of 0.1 ms in order to achieve optimum control performance and efficient utilization of computing resources. It is recommended that the sampling time be approximately one-tenth of the constant of the dominant process time [38]. It is important to note that the parameter n (representing the number of motor rotation steps) is a variable in this context, and for this simulation, it is set to $n = 800$. Then $K_p^{'} = \dfrac{2 \cdot 0.25 \cdot 0.01}{35} \cdot 800 = 0.1143$.

Simulation Parameters: SIMC-PID Skogestad Tuning. By implementing the SIMC-PID Skogestad tuning methodology for an integral process [30], we derive the subsequent parameters for the PI controller; they read

$$K = \frac{1}{K_p^{'}} \cdot \frac{1}{\tau_c + \theta}, \qquad T_i = 4(\tau_c + \theta). \tag{20}$$

Here K is the proportional gain, $K_p^{'}$ is the integral process gain, τ_c is the closed loop time constant, θ is the delay (equal to zero in our case), and T_i is the integral time. Therefore, the computation leads to $K = 2.91$ and $T_i = 12$, with $K_p^{'} = 0.1143$, $\theta = 0$, and $\tau_c = 3$. Note, that a compromise between performance and robustness requires a medium τ_c (neither small value nor big).

DMC Parameters: $P = 10$, $m = 5$, $\alpha = 0.6$, and $\lambda = 0.6$. Simulation time T = [350, 1600, and 1500] is allocated for three different scenarios, namely, a constant trajectory, a variable trajectory, and the presence of disturbance. The constant trajectory $w(t) = 5$ and the variable trajectory are implemented as step changes in both upward and downward directions. The effectiveness of the DMC technique is assessed in the context of the mentioned scenarios, and it is compared to the SIMC-PID approach proposed by Skogestad. This evaluation is conducted by examining Figs. 6–9.

In Fig. 6 a, b, the performance of both the MPC and SIMC-PID controllers, with no position error, is analyzed with respect to the angle of the beam rotation (i.e., the output). Initially, oscillations in the output are observed for a duration of 250 samples or 25 ms, before it stabilizes with the DMC controller; see Fig. 6 a. The SIMC-PID and DMC controllers exhibit favorable behavior, except for a brief peak at the beginning; see Fig. 6 a. A duration of 250 samples is deemed satisfactory for the static alignment operation without laser beam emission. However, in dynamic scenarios, where the laser beam is emitted at intervals of 50 ms between shots, the oscillation period must be reduced to less than 5 ms, using the DMC controller. In contrast, the SIMC-PID controller overcomes this issue effectively; see Fig. 6 b, as the control operation is one of several operations in the chain.

In Fig. 6 c, we present the evolution of the angle motor rotation u (the input). The rotating motor is responsible for exerting this rotation. Initially, an oscillation is observed at the commencement of the movement, lasting for 250 samples or 25 ms. Subsequently, the motor movement becomes stable with the MPC controller; see Fig. 6 c. In terms of control input u, the SIMC-PID exhibits a smooth behavior, except for the initial peak. However, compared to the DMC controller, the SIMC-PID requires a larger amplitude value to effectively control the system; see Fig. 6 d, which is not the case with the DMC controller.

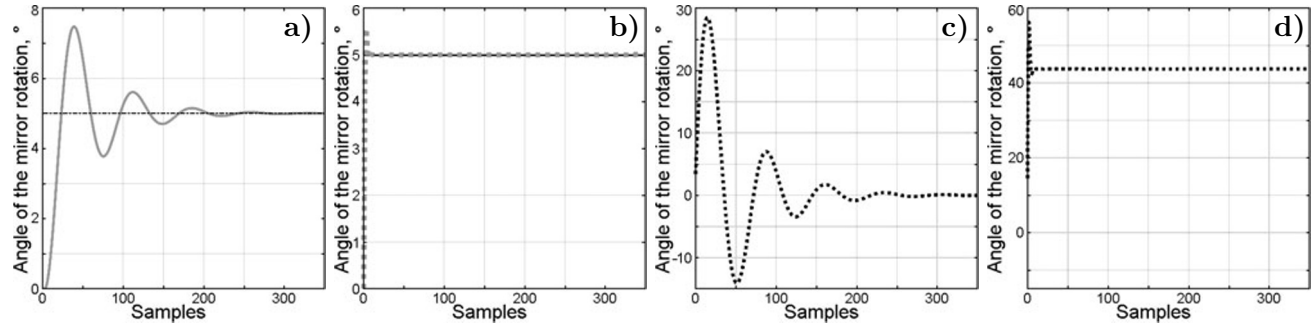

Fig. 6. Mirror alignment position (output θ) with DMC (a) and with SIMC-PID (b). Rotation of the motor shaft (input u) with DMC (c) and with SIMC-PID (d).

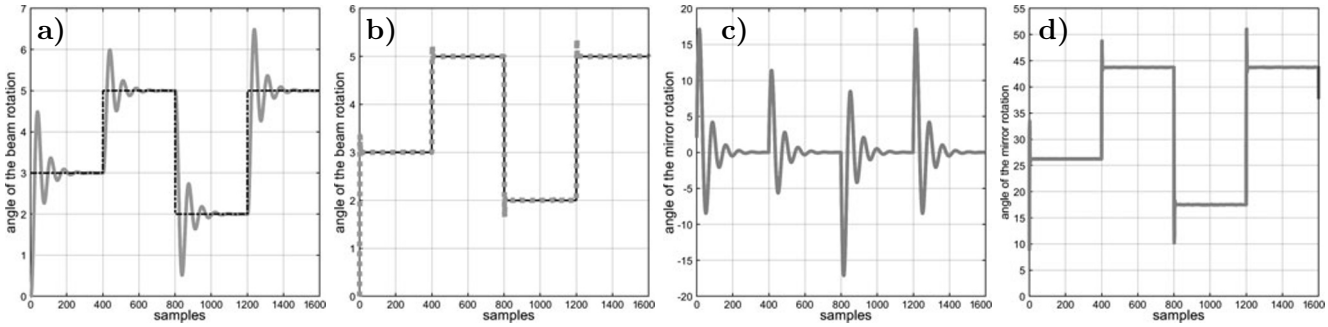

Fig. 7. The output θ with DMC (a) and with SIMC-PID (b). Rotation of the motor shaft (input u) with DMC (c) and with SIMC-PID (d), variable reference case.

In Fig. 7, we analyze the monitoring of the anticipated outcome for a variable trajectory. Before the stabilization, a diminishing oscillation is observed with each variation of the trajectory, when utilizing the DMC controller; see Fig. 7 a. Conversely, the SIMC-PID controller; see Fig. 7 b, expedites the attainment of the trajectory's final value, thus, granting it a higher priority compared to the DMC controller.

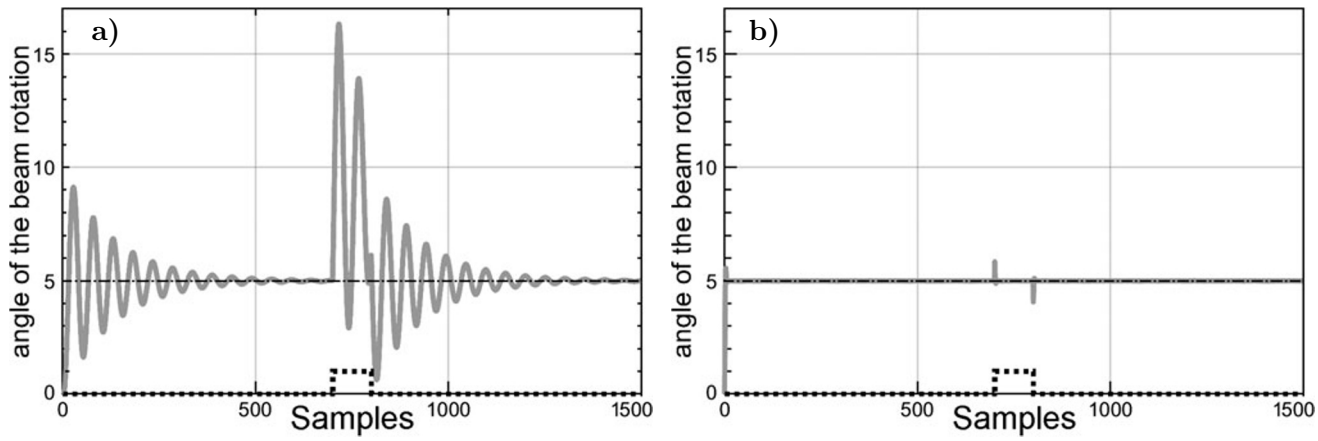

Fig. 8. The output of the system in the presence of disturbance with DMC (a) and with SIMC-PID (b). Here, desired output (dash-dotted curves), disturbance (dotted curves), and θ output (solid curves).

When considering the variable trajectory, the input of the system is enhanced, when employing the DMC controller (Fig. 7 c) in contrast to the SIMC-PID controller (Fig. 7 d). Despite the presence of oscillation with the DMC controller, the system is still able to perform better with it, due to the allowable energy requirement.

The final examination shown in Fig. 8 is conducted in the event of the existence of a perturbation. It occurs in the configuration of pattern 700 for one hundred samples; see Fig. 8 and influences the functioning of the system by inducing vibrations that deviate from the desired response at a magnitude of 16. Subsequently, these deviations are mitigated and completely eliminated through the utilization of the proposed controllers; see Fig. 8. The performance of the output, using the SIMC-PID controller, is exceptional, as it swiftly rejects the disturbance as soon as it emerges; see Fig. 8 b, in contrast to the DMC controller, which necessitated a greater amount of time; see Fig. 8 a.

In Fig. 9, we see that the input initially exhibits excessive vigor, when the disturbance arises, before eventually transiting into a smoother trajectory with the aid of the DMC controller; see Fig. 9 a. Conversely, the input demonstrates a smooth behavior with the SIMC-PID controller, which can be attributed to its prompt rejection of the disturbance. Nevertheless, it maintains a considerable magnitude that exceeds 40 in terms of amplitude, which can be perceived as a drawback; see Fig. 9 b.

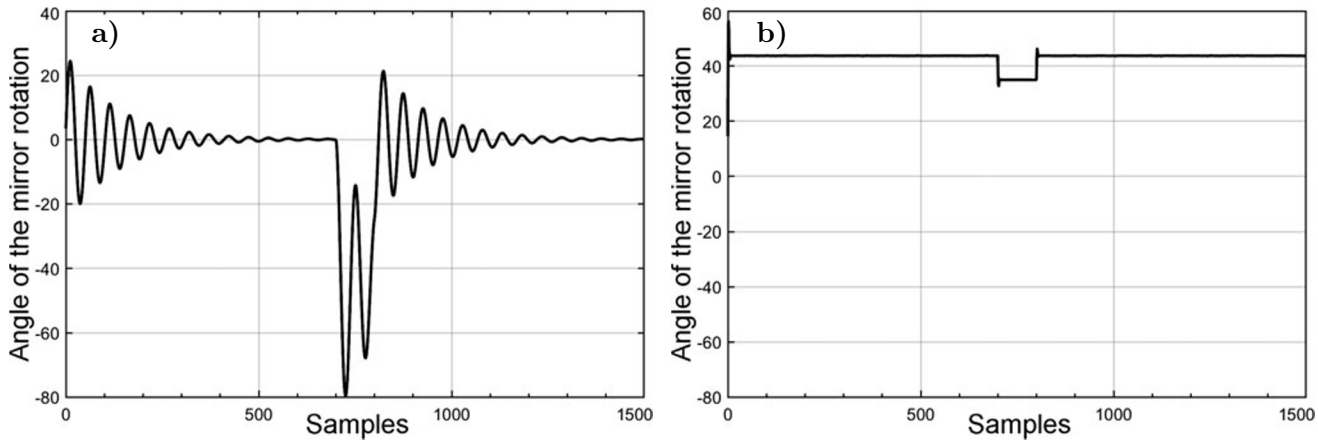

Fig. 9. The input of the system in the presence of disturbance with DMC (a) and with SIMC-PID (b).

5. Conclusions

Based on the modeling of a LiDAR system's optical chain, we subjected the integration system's transfer function to two controllers. With a brief overview of the LiDAR system utilized for forest fire detection and atmospheric analysis, the optical chain was modeled and visually represented through various figures. We presented the Dynamic Matrix Control (DMC) algorithm's theoretical development, which employed the step response. The fundamental principle of predictive control lied in the establishment of an anticipatory effect. The explicit knowledge of the future trajectory's evolution was exploited and compared with the SIMC-PID Skogestad controller through simulation. The simulation results, which examined constant trajectory, variable trajectory, and the presence of disturbances, demonstrated stable behavior and commendable performance for this intricate system with the proposed pair of controllers. Despite the existence of external disturbances, they effectively maintained the desired behavior and achieved the desired set point and reference value, with a preference for SIMC-PID for output and DMC for input. The obtained results from the proposed technique successfully addressed the raised issue, enabling accurate manipulation of alignment in similar systems, saving time, and swiftly returning to the preferred alignment for the mobile LiDAR system to function correctly.

References

1. A. Pozzi and D. M. Raimondo, *J. Energy Storage*, **55, Part A**, 105332 (2022); DOI: 10.1016/j.est.2022.105332
2. A. Ramdani, "Commande Prédictive des Systèmes Dynamiques Étude Comparative avec les Régulateurs Classiques," Magister Dissertation, Dept. Auto. Elect. Indust. Pros., The M'Hamed Bougara University of Boumerdes, Boumerdes (2013).
3. J. ElHadj Ali, E. Feki, and A. Mami, *Int. J. Adv. Comput. Sci. Appl.*, **10**, 0100646 (2019); DOI: 10.14569/IJACSA.2019.0100646
4. A. Pawlowski, M. Schiavo, N. Latronico, et al., *J. Process Control*, **117**, 98 (2022); DOI: 10.1016/j.jprocont.2022.07.007
5. S. Yuan, Z. Liu, L. Zheng, et al., *Ocean Eng.*, **258**, 111082 (2022); DOI: 10.1016/j.oceaneng.2022.111082
6. R. Chai, A. Tsourdos, H. Gao, et al., *Automatica*, **145**, 110561 (2022); DOI: 10.1016/j.automatica.2022.110561
7. A. Ramdani and M. Traiche, *Math. Sci. Eng. Aerosp.*, **13**, 441 (2022).
8. Y. Zhu, W. Yan, and Y. Zhu, *J. Process Control*, **106**, 122 (2021); DOI: 10.1016/J.JPROCONT.2021.08.018
9. M. Schulze and D. Gerrit, "On Closed-Loop Dynamics of ADMM-Based MPC," arXiv: Optimization and Control, in: T. Faulwasser, M. A. Müller, and K. Worthmann (Eds.), *Recent Advances in Model Predictive Control*, Lecture Notes in Control and Information Sciences, Springer, Cham (2021), Vol. 485, pp. 107–134; DOI: 10.1007/978-3-030-63281-6_5
10. H. Li and C. L. E. Swartz, *Comput. Ch. Eng.*, **122**, 356 (2019); DOI: 10.1016/J.COMPCHEMENG.2018.08.028
11. K. Worthmann, M. W. Mehrez, G. K. I. Mann, et al., *Automatica*, **82**, 243 (2017); DOI: 10.1016/J.AUTOMATICA.2017.04.038
12. N. M. Abbas, *Int. J. Appl. Power Eng.*, **10**, 244 (2021); DOI: 10.11591/IJAPE.V10.I3.PP244-252
13. Z. Lammouchi and K. Barra, *Int. J. Appl. Power Eng.*, **4**, 104 (2015); DOI: 10.11591/IJAPE.V4.I3.PP104-117
14. I. González-Torres, H. Miranda, C. Méndez-Barrios, et al., "Dynamic matrix predictive control on DC-AC modular multilevel converter: Design, control and realtime simulation," in: 2017 IEEE Energy Conversion Congress and Exposition (ECCE), Cincinnati, OH, USA (2017), pp. 4552-4559; DOI: 10.1109/ECCE.2017.8096780
15. W. Chang, W. Dong, L. Zhao, and Y. Qiang, "Model predictive control-based energy collaborative optimization management for energy storage system of virtual power plant," in: 2020 19th International Symposium on

Distributed Computing and Applications for Business Engineering and Science (DCABES), Xuzhou, China (2020), pp. 112-115; DOI: 10.1109/DCABES50732.2020.00037
16. Z. Ding, Z. Yang, C. Chen, et al., *Mech. Syst. Signal Process.*, **167, Part A**, 108543 (2022); DOI: 10.1016/J.YMSSP.2021.108543
17. L. Andong, J. Peng, Z. Wenan, et al., "Dynamic Matrix Control Method for Networked System Having Time Delay and Packet Loss," Patent CN105353622A, Zhejiang University of Technology (2016).
18. Z. Wen-jie, *Dynamic Matrix Control Algorithm Design and Simulation Based on MATLAB*, Electronic Instrumentation Customers (2012).
19. Q. Hong, Y. Yuan, Z. Dongliang, et al., "Dynamic Matrix Control Method for Controlled Object with Integrals and Delay Link," Shanghai University of Electric Power (2018).
20. G. Lu, Y. Lu, T. Deng, and H. Liu, "Automatic alignment of optical-beam-based GPS for free-space laser communication system," in: Free-Space Laser Communication and Active Laser Illumination III (2004); *Proc. SPIE*, **5160**; DOI: 10.1117/12.507410
21. E. Morrison, B. J. Meers, D. I. Robertson, and H. Ward, *Appl. Opt.*, **33**, 5041 (1994); DOI: 10.1364/AO.33.005041
22. Q. Fu, P. Tan, K. F. Liu, et al., *Infrared Phys. Technol.*, **91**, 187 (2018); DOI: 10.1016/j.infrared.2018.04.009
23. X. Liu, K. Liu, B. Qin, et al., *Nucl. Instrum. Methods. Phys. Res. A*, **837**, 58 (2016); DOI: 10.1016/j.nima.2016.08.043
24. X. Liu, J. Guo, G. Li, et al., *Results Phys.*, **12**, 1044 (2019); DOI: 10.1016/j.rinp.2018.12.071
25. A. Sharma, V. Sivakumar, C. Bollig, et al., *S. Afr. J. Sci.*, **105**, 456 (2009); `journals.co.za/doi/pdf/10.10520/EJC96853`
26. L. Shikwambana and V. Sivakumar, "Aerosol optical depth measurements over Pretoria using CSIR Lidar and sun-photometer: A case study," in: *30th Annual Conference of South African Society For Atmospheric Sciences. Modeling and Observation of the Atmosphere, Proceedings of the Reviewed Papers, 01–02 Oct. 2014*, pp. 138-141.
27. L. Shikwambana and V. Sivakumar, "Observation of clouds using the CSIR transportable LiDAR: A case study over Durban, South Africa," *Adv. Meteorol.*, **2016**, 4184512 (2016); DOI: 10.1155/2016/4184512
28. P. Weibring, H. Edner, and S. Svanberg, *Appl. Opt.*, **42**, 3583 (2003); DOI: 10.1364/ao.42.003583
29. M. Traïche and A. Kedadra, "A Dual LiDAR System for Environmental Studies," Society for Photo-Optical Instrumentation Engineers SPIE Newsroom 4801 (2013); DOI: 10.1117/2.1201306.004801
30. S. Sigurd, *J. Process Control*, **13**, 291 (2003); DOI: 10.1016/S0959-1524(02)00062-8
31. C. R. Cutler and P. S. Ramaker, "Dynamic matrix control — A computer algorithm," in: Proceedings of the Joint Automatic Control Conference, San Francisco, CA, USA (1980); paper No. WP5-B; DOI: 10.1109/JACC.1980.4232009
32. S. J. Qin and T. A. Badgwell, *Control Eng. Pract.*, **11**, 733 (2003); DOI: 10.1016/S0967-0661(02)00186-7
33. P. Tatjewski, *Advanced Control of Industrial Processes: Structures and Algorithms*, Springer Science & Business Media, London (2007).
34. A. Ramdani, S. Grouni, and K. Bouallegue, *Advanced Trajectory Tracking Control Applied to Dynamic System with Disturbance*, International Publisher & C.O (IPCO) (2014). pp.120-128.
35. E. Seborg, T. F. Edgar, D. A. Mellichamp, and F. J. Doyle, *Process Dynamics and Control*, International Student Version, Wiley (2011), 3rd ed.
36. E. F. Camacho and C. Bordons, "Model predictive controllers," in: *Model Predictive control. Advanced Textbooks in Control and Signal Processing*, Springer, London (2007); DOI: 10.1007/978-0-85729-398-5_2
37. A. Ramdani, Elaboration des Techniques de Commandes Prédictives: Application à une Chaine Optique, Ph.D. Theses, Dept. Auto. Elect. Indust. Proc., The M'Hamed Bougara Univ. of Boumerdes., Boumerdes (2018).
38. C. A. Smith and A. B. Corripio, *Principles and Practice of Automatic Process Control*, Wiley (1997), 2nd ed.